Is Ferromagnetism an Intrinsic Property of the Cu^{II}/Gd^{III} Couple? 2. Structures and Magnetic Properties of Novel Trinuclear Complexes with μ-Phenolato-μ-oximato (Cu−Ln−Cu) Cores (Ln = La, Ce, Gd)

Jean-Pierre Costes,* Françoise Dahan, and Arnaud Dupuis

Laboratoire de Chimie de Coordination du CNRS, UPR 8241, liée par conventions à l'Université Paul Sabatier et à l'Institut National Polytechnique de Toulouse, 205 route de Narbonne, 31077 Toulouse Cedex, France

Received June 20, 2000

The present paper is devoted to the study of original trinuclear (Cu^{II}, Ln^{III}, Cu^{II}) complexes (Ln = La, Ce, Gd). They derive from the polydentate ligands H_2L^i (i = 1, 3, 4) represented in Figure 1. The crystal and molecular structures of two complexes have been determined at room temperature. The (Cu, Gd, Cu) complex of H_2L^1 **1Gd** and the (Cu, Ce, Cu) complex of H_2L^3 **3Ce** crystallize in the triclinic space group $P\bar{1}$ (no. 2) with the following cell parameters: a = 14.005(2) Å, b = 14.7581(13) Å, c = 11.3549(13) Å, α = 96.273(9)°, β = 97.648(11)°, γ = 72.946(9)°, V = 2217.7(4) Å^3, and Z = 2 for **1Gd** and a = 11.226(2) Å, b = 16.927(3) Å, c = 11.010(2) Å, α = 108.67(2)°, β = 110.48(1)°, γ = 92.35(2)°, V = 1828.7(5) Å^3, and Z = 2 for **3Ce**. Regarding possible supports for magnetic interactions, it may be noted that, in both complexes, each of the main bridging pathways between the equatorial positions of a copper(II) ion and the related lanthanide ion is double and not symmetrical. It involves a phenolato oxygen atom and an oximato nitrogen−oxygen pair of atoms. The resulting Cu(O,N−O)Gd networks are not planar, but **3Ce** displays much larger deviations than does **1Gd**. Determination of the thermal dependence of χ_M (molar susceptibility) and the field variations of M (magnetization) show that in **3Gd** and **4Gd** the Cu−Gd interactions are antiferromagnetic while more "usual" ferromagnetic interactions are observed for **1Gd**. The possibility of a relationship between structural and magnetic parameters is considered.

Introduction

In a recent paper,[1] we have described two binuclear (Cu, Gd) complexes (**1′Gd** and **2′Gd** in Figure 1), which despite their formal resemblance exhibit significantly different magnetic properties. The Cu−Gd interaction which, in both cases, is mediated by a double (O, N−O) bridge is ferromagnetic in **1′Gd** but antiferromagnetic in **2′Gd**. The latter behavior is unprecedented since all the previously reported complexes involving CuO_2Gd [2−15] and Cu(O,N−O)Gd cores [1,16,17] are ferromagnetic. Scrutinizing the structural data shows that the most pertinent difference between **1′Gd** and **2′Gd** concerns the Cu(O,N−O)-Gd bridging network which is almost planar in the former complex and bent in the latter one. These results prompt us to enlarge our study to the trinuclear (Cu, Ln, Cu) complexes prepared from the polydentate ligands H_2L^i (i = 1,3, and 4, cf. Figure 1). The experimental data support further the view that the Cu−Gd interaction mediated by a (O, N−O) double bridge may be either ferromagnetic or antiferromagnetic, depending on the degree of planarity of the bridging core. Relevant to the present study we may note two very recent papers.[18,19] They report on the occurrence of antiferromagnetic interactions in gadolinium−organic radical derivatives.

Experimental Section

Materials and Methods. All starting materials were purchased from Aldrich and were used without further purification. $Cu(SalOMe)_2$, L^1-Cu, L^4Cu, and L^4Ni complexes and 1-(2,4,4-trimethyl-2-imidazolidinyl)-1-ethanone oxime ligand were obtained as previously described.[1,14,20,21] New complexes are described hereafter.

* Corresponding author. E-mail: costes@lcc-toulouse.fr.

(1) Costes, J. P.; Dahan, F.; Dupuis, A.; Laurent, J. P. *Inorg. Chem.* **2000**, *39*, 169.
(2) Bencini, A.; Benelli, C.; Caneschi, A.; Carlin, R. L.; Dei, A.; Gatteschi, D. *J. Am. Chem. Soc.* **1985**, *107*, 8128.
(3) Bencini, A.; Benelli, C.; Caneschi, A.; Dei, A.; Gatteschi, D. *Inorg. Chem.* **1986**, *25*, 572.
(4) Bencini, A.; Benelli, C.; Caneschi, A.; Gatteschi, D.; Pardi, L. *Inorg. Chem.* **1990**, *29*, 1750.
(5) Matsumoto, N.; Sakamoto, M.; Tamaki, H.; Okawa, H.; Kida, S. *Chem. Lett.* **1990**, 853.
(6) Sakamoto, M.; Hashimura, M.; Matsuki, K.; Matsumoto, N.; Inoue, K.; Okawa, H. *Bull. Chem. Soc. Jpn.* **1991**, *64*, 3639.
(7) Guillou, O.; Bergerat, P.; Kahn, O.; Bakalbassis, E.; Boubekeur, K.; Batail, P.; Guillot, M. *Inorg. Chem.* **1992**, *31*, 110.
(8) Guillou, O.; Oushoorn, R. L.; Kahn, O.; Boubekeur, K.; Batail, P. *Angew. Chem., Int. Ed. Engl.* **1992**, *31*, 626.
(9) Andruh, M.; Ramade, I.; Codjovi, E.; Guillou, O.; Kahn, O.; Trombe, J. C. *J. Am. Chem. Soc.* **1993**, *115*, 1822.
(10) Blake, A. J.; Milne, P. E. Y.; Thornton, P.; Winpenny, R. E. P. *Angew. Chem., Int. Ed. Engl.* **1991**, *30*, 1139.
(11) Bouayad, A.; Brouca-Cabarrecq, C.; Trombe, J. C.; Gleizes, A. *Inorg. Chim. Acta* **1992**, *195*, 193.
(12) Costes, J. P.; Dahan, F.; Dupuis, A.; Laurent, J. P. *Inorg. Chem.* **1996**, *35*, 2400.
(13) Ramade, I.; Kahn, O.; Jeannin, Y.; Robert, F. *Inorg. Chem.* **1997**, *36*, 930.
(14) Costes, J. P.; Dahan, F.; Dupuis, A.; Laurent, J. P. *Inorg. Chem.* **1997**, *36*, 3429.
(15) Costes, J. P.; Dahan, F.; Dupuis, A.; Laurent, J. P. *New J. Chem.* **1998**, 1525.
(16) Benelli, C.; Blake, A. J.; Milne, P. E. Y.; Rawson, J. M.; Winpenny, R. E. P. *Chem. Eur. J.* **1995**, *1*, 614.
(17) Stemmler, A. J.; Kampf, J. W.; Kirk, M. L.; Atasi, B. H.; Pecoraro, V. L. *Inorg. Chem.* **1998**, *37*, 2807.
(18) Lescop, C.; Luneau, D.; Belorisky, E.; Fries, P.; Guillot, M.; Rey, P. *Inorg. Chem.* **1999**, *38*, 5472.
(19) Caneschi, A.; Dei, A.; Gatteschi, D.; Sorace, L.; Vostrikova, K. *Angew. Chem., Int. Ed. Engl.* **2000**, *39*, 246.

10.1021/ic000666u CCC: $19.00
Published on Web 11/30/2000

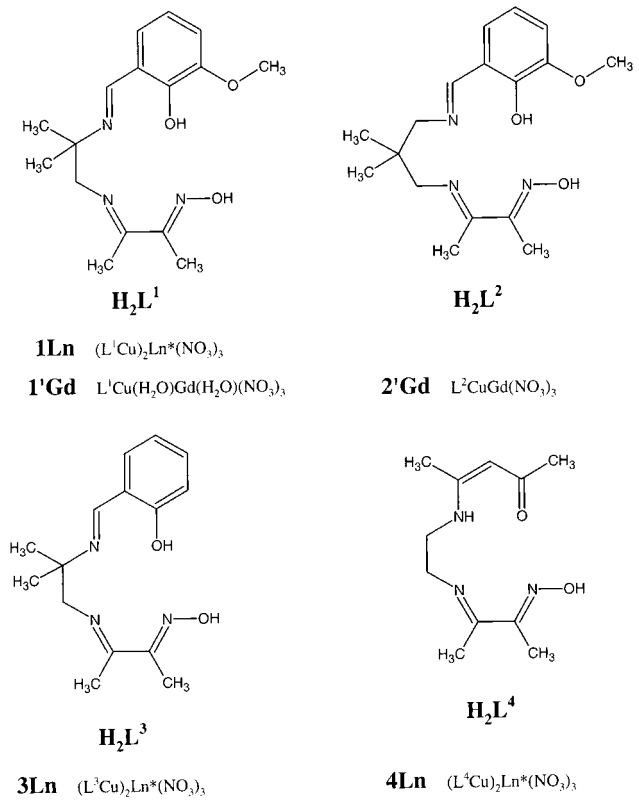

Figure 1. Schematic representation of the ligands used in this work (Ln = La, Ce, or Gd).

L^3Cu. A mixture of $Cu(SalOMe)_2$ (1.83 g, 5×10^{-3} mol) and of 1-(2,4,4-trimethyl-2-imidazolidinyl)-1-ethanone oxime (0.85 g, 5×10^{-3} mol) in acetone (20 mL) was heated for 10 min and then left to cool with stirring. The precipitate that appeared was filtered off and washed with acetone and diethyl ether. Yield: 1.6 g (95%). Anal. Calcd for $C_{15}H_{19}CuN_3O_2$: C, 53.5; H, 5.7; N, 12.5. Found: C, 53.4; H, 5.6; N, 12.4. Mass spectrum (FAB^+, 3-nitrobenzyl alcohol matrix): $m/z = 337$, $[L^3Cu + 1]^+$.

Trinuclear Complexes. As the experimental procedures are quite similar, we will only describe the detailed preparation of one of them while analytical results will be reported for the entire set of complexes.

$(L^3Cu)_2Gd(NO_3)_3$. 3Gd. A mixture of L^3Cu (0.67 g, 2×10^{-3} mol) and $Gd(NO_3)_3 \cdot 5H_2O$ (0.43 g, 1×10^{-3} mol) in acetone (10 mL) was heated for 10 min and then left to cool with stirring. The precipitate that appeared was filtered off and washed with acetone and diethyl ether. Yield: 0.81 g (80%). Anal. Calcd for $C_{30}H_{38}Cu_2GdN_9O_{13}$: C, 35.4; H, 3.8; N, 12.4. Found: C, 35.1; H, 3.6; N, 12.1. Mass spectrum (FAB^+, 3-nitrobenzyl alcohol matrix): $m/z = 956$, $[(L^3Cu)_2Gd(NO_3)_2]^+$.

$(L^3Cu)_2Ce(NO_3)_3$. 3Ce. Anal. Calcd for $C_{30}H_{38}CeCu_2N_9O_{13}$: C, 36.0; H, 3.8; N, 12.6. Found: C, 35.6; H, 3.4; N, 12.3. Mass spectrum (FAB^+, 3-nitrobenzyl alcohol matrix): $m/z = 938$, $[(L^3Cu)_2Ce(NO_3)_2]^+$. Crystals were obtained by slow evaporation of the mother solution.

$(L^3Cu)_2La(NO_3)_3 \cdot 2H_2O$. 3La. Anal. Calcd for $C_{30}H_{38}Cu_2LaN_9O_{13} \cdot 2H_2O$: C, 35.4; H, 4.0; N, 12.4. Found: C, 34.9; H, 4.1; N, 12.3. Mass spectrum (FAB^+, 3-nitrobenzyl alcohol matrix): $m/z = 935$, $[(L^3Cu)_2La(NO_3)_2]^+$.

$(L^4Cu)_2Gd(NO_3)_3$. 4Gd. Anal. Calcd for $C_{22}H_{34}Cu_2GdN_9O_{13}$: C, 28.8; H, 3.7; N, 13.7. Found: C, 28.8; H, 3.5; N, 13.6. Mass spectrum (FAB^+, 3-nitrobenzyl alcohol matrix): $m/z = 856$, $[(L^4Cu)_2Gd(NO_3)_2]^+$.

$(L^4Cu)_2La(NO_3)_3$. 4La. Anal. Calcd for $C_{22}H_{34}Cu_2LaN_9O_{13} \cdot C_3H_6O$: C, 31.4; H, 4.2; N, 13.2. Found: C, 31.5; H, 4.1; N, 13.2. Mass spectrum (FAB^+, 3-nitrobenzyl alcohol matrix): $m/z = 836$, $[(L^4Cu)_2La(NO_3)_2]^+$.

Table 1. Crystallographic Data for **1Gd** and **3Ce**

	1Gd	3Ce
chem. formula	$C_{32}H_{52}Cu_2GdN_9O_{20}$	$C_{30}H_{38}CeCu_2N_9O_{13}$
fw	1167.16	999.89
space group	$P\bar{1}$ (no. 2)	$P\bar{1}$ (no. 2)
a, Å	14.005(2)	11.226(2)
b, Å	14.7581(13)	16.927(3)
c, Å	11.3549(13)	11.010(2)
α, deg	96.273(9)	108.67(2)
β, deg	97.648(11)	110.48(1)
γ, deg	72.946(9)	92.35(2)
V, Å^3	2217.7(4)	1828.7(5)
Z	2	2
ρ_{calcd}, g cm^{-3}	1.748	1.816
λ, Å	0.71073	0.71073
T, K	293	293
μ(Mo Kα) cm^{-1}	25.15	24.53
R^a	0.0253, 0.0326	0.0332, 0.0442
Rw^b	0.0643, 0.0701	0.0862, 0.0957

[a] $R = \sum||Fo| - |Fc||/\sum|Fo|$. [b] $R_w = [\sum[w(|Fo|^2 - |Fc|^2)^2]/\sum w|Fo^2|^2]^{1/2}$.

$(L^1Cu)_2Gd(NO_3)_3 \cdot 3H_2O$. 1Gd. This complex was directly obtained as crystals from the solution mixture by slow evaporation. Anal. Calcd for $C_{32}H_{48}Cu_2GdN_9O_{18}$: C, 35.4; H, 4.0; N, 12.4. Found: C, 34.9; H, 4.1; N, 12.3. Mass spectrum (FAB^+, 3-nitrobenzyl alcohol matrix): $m/z = 1016$, $[(L^1Cu)_2Gd(NO_3)_2]^+$.

Methods. Elemental analyses were carried out by the Service de Microanalyse du Laboratoire de Chimie de Coordination, Toulouse (C, H, N). Magnetic susceptibility data were collected on powdered samples of the different compounds with use of a SQUID-based sample magnetometer on a QUANTUM Design Model MPMS instrument. All data were corrected for diamagnetism of the ligands estimated from Pascal's constants.[22] Positive FAB mass spectra were recorded in DMF as a solvent and 3-nitrobenzyl alcohol matrix with a Nermag R10-10 spectrometer.

X-ray Crystallographic Procedures. Crystal data for **1Gd** and **3Ce** are presented in Table 1. Data were measured on an Enraf-Nonius CAD4 diffractometer with Mo Kα ($\lambda = 0.710\,73$ Å) radiation and $\omega - 2\theta$ scans. The temperature of measurement was 293 K. The reflections were corrected for Lorentz-polarization effects with the MolEN package.[23] Semiempirical absorption corrections[24] based on ψ scans were applied. The structures were solved using a Patterson procedure with the SHELXS-97 program[25] and refined against all Fo^2 (SHELXL-97)[26] with a weighting scheme $w^{-1} = \sigma^2(Fo^2) + (aP)^2 + bP$, where $3P = (Fo^2 + 2Fc^2)$ and *a* and *b* are constants adjusted by the program. All non-hydrogen atoms were refined anisotropically. Hydrogen atoms were included using a riding model with *U* equal to 1.1 times U_{eq} of atom of attachment, except those bonded to the water molecules in **1Gd**, which were allowed to vary isotropically. Atomic scattering factors were taken from a standard source.[27] Structures were drawn with the ZORTEP[28] program. Selected fractional coordinates are given in Tables 2 (**1Gd**) and 3 (**3Ce**).

Results and Discussion

The original complexes (**1Ln**, **3Ln**, and **4Ln** with Ln = Gd, La, Ce) described in the present work are trinuclear with a

(20) Costes, J. P.; Dahan, F.; Dupuis, A.; Laurent, J. P. *J. Chem. Soc., Dalton Trans.* **1998**, 1307.
(21) Costes, J. P.; Dahan, F.; Dupuis, A.; Laurent, J. P. *New J. Chem.* **1997**, *21*, 1211.
(22) Pascal, P. *Ann. Chim. Phys.* **1910**, *19*, 5.
(23) Fair, C. K. *MolEN. Structure Solution Procedures*; Enraf-Nonius: Delft, Holland, 1990.
(24) North, A. C. T.; Phillips, D. C.; Mathews, F. S. *Acta Crystallogr., Sect. A* **1968**, *A24*, 351.
(25) Sheldrick, G. M. *SHELXS-97. Program for Crystal Structure Solution*; University of Göttingen: Göttingen, Germany, 1990.
(26) Sheldrick, G. M. *SHELXL-97. Program for the refinement of crystal structures from diffraction data*; University of Göttingen: Göttingen, Germany, 1997.
(27) *International Tables for Crystallography*; Kluwer Academic Publishers: Dordrecht, The Netherlands, 1992; Vol. C.
(28) Zsolnai, L.; Pritzkow, H.; Huttner, G. *ZORTEP. Ortep for PC, Program for Molecular Graphics*; University of Heidelberg, Heidelberg, Germany, 1996.

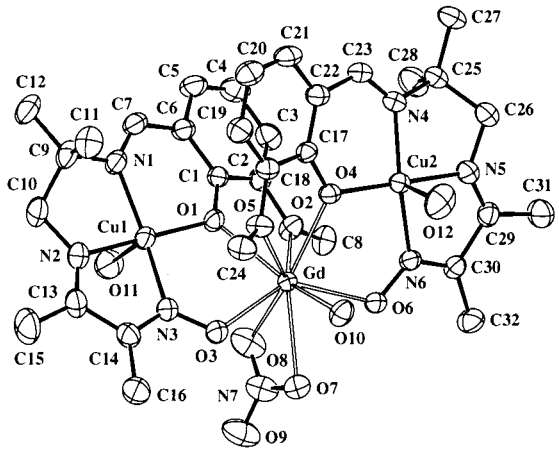

Figure 2. Zortep plot for **1Gd** with ellipsoids drawn at the 50% probability level.

Cu(O,N−O)Ln(O,N−O)Cu core while the previously reported complexes[1] (**1′Gd** and **2′Gd**) are binuclear. It may be noted that the H_2L^1 ligand may lead to a binuclear **1′Gd** or a trinuclear **1Gd** complex depending on the ratio of reactants. By contrast, H_2L^3 and H_2L^4 only yield trinuclear species while a binuclear complex is solely obtained from H_2L^2. Relevant to the present study are the works quoted in refs 16 and 17. They concern polynuclear Cu_nL_n complexes involving 5-chloropyridone as ligand and metallacrown complexes, respectively. Both types of compounds include bridging networks of the Cu(O,N−O)-Ln sort.

From the data of chemical analysis and mass (FAB^+) spectroscopy, the complexes under study may be represented by the formulas $L^1{}_2Cu_2Gd(H_2O)_3(NO_3)_3$ and $L^i{}_2Cu_2Ln(NO_3)_3$ ($i = 3$ and 4; Ln = Gd, La, Ce). Almost identical FAB^+ spectra were obtained for the homologous complexes of H_2L^3 and H_2L^4 with signals attributable to the $[(L^iCu)_2Ln(NO_3)_2]^+$ (100%) and $[L^iCuLn(NO_3)_2]^+$ (15−20%) species in both series ($i = 3$ and 4). Crystal and molecular structures were determined by X-ray crystallographic analysis in the case of **1Gd** and **3Ce** for which appropriate crystals have been obtained.

Description of the 1Gd Structure. One distinctive feature of the **1Gd** structure is that the trinuclear network is not neutral but dicationic. It is well represented by the formula $[(L^1Cu(H_2O))_2Gd(H_2O)(NO_3)]^{2+}$. In addition to two trinuclear entities, the unit cell contains four uncoordinated nitrato ions and four unbound water molecules. A view of the bimetallic cation is represented in Figure 2 while relevant bond lengths and angles of the Cu(II) and Gd(III) environments are quoted in Table 4. The cation has no crystallographic symmetry; the bond lengths and angles of the two $(L^1Cu)Gd/2$ moieties differ little.

The central gadolinium ion is linked to each copper ion by a double (O, N−O) bridge (O standing for the phenolato oxygen atom and N−O for the oximato group of the L^1 ligand). The five atoms involved in each Cu(O,N−O)Gd bridge are not exactly coplanar. The dihedral angles (α) between the (OCuN) and (OGdO) planes are equal to 7.3(3)° and 8.8(2)° in the Cu(1) and Cu(2) moieties, respectively. The related Cu···Gd separations are equal to 3.6388(4) and 3.6328(3) Å. A sort of third bridge results from the fact that each OMe sidearm which intrinsically belongs to the mononuclear (L^1Cu) entity is coordinated to the Gd ion. The polyatomic pathway which connects the two metal ions is too extended to support a significant magnetic interaction but, it can contribute to the stability of the trinuclear species.

The gadolinium ion is nine-coordinated. In addition to the six oxygen atoms afforded by two L^1 ligands, the rare earth ion achieves its environment with three oxygen atoms coming from a bidentate (η^2-coordination) nitrato ion and a water molecule. As previously noted, the Gd−O bond lengths depend on the nature of the oxygen atoms; they vary from 2.371(2) to 2.620(2) Å with a mean value of 2.460 Å. The bonds issued from the oximato and phenolato oxygens are shorter than those from the water molecules, the largest ones being related to the methoxy sidearms and the nitrato ions.

Each copper ion has a classical square-pyramidal environment. The four basal donors (N_3O) are afforded by a L^1 ligand, while a water molecule occupies the apical position. As usual, the apical Cu−O bonds with a mean value of 2.357 Å are longer than the equatorial ones (mean value 1.908 Å).

Table 2. Selected Atomic Coordinates and Equivalent Isotropic Displacement Parameters (Å^2 × 100) for $[\{L^1Cu(H_2O)\}_2Gd(H_2O)(NO_3)](NO_3)_2\ (H_2O)_2$, **1Gd**

atom	*x/a*	*y/b*	*z/c*	U_{eq}[a]
Gd	0.34209(1)	0.44952(1)	0.11235(1)	2.470(4)
Cu(1)	0.26063(2)	0.27275(2)	0.24048(3)	3.328(7)
Cu(2)	0.26549(2)	0.70079(2)	0.20899(2)	3.283(7)
O(1)	0.2218(1)	0.4017(1)	0.1998(1)	2.99(3)
O(2)	0.1541(1)	0.5392(1)	0.0629(2)	3.46(4)
O(3)	0.4256(1)	0.2869(1)	0.1142(2)	3.65(4)
O(4)	0.2967(1)	0.5759(1)	0.2608(1)	3.00(3)
O(5)	0.4076(1)	0.4161(1)	0.3349(1)	3.68(4)
O(6)	0.3423(1)	0.5774(1)	−0.0016(1)	3.15(3)
O(7)	0.4311(2)	0.3831(1)	−0.0748(2)	4.98(5)
O(8)	0.2808(2)	0.3737(2)	−0.0763(2)	6.96(7)
O(9)	0.3774(2)	0.2866(3)	−0.2046(3)	9.8(1)
O(10)	0.5088(1)	0.4690(2)	0.1570(2)	4.03(4)
O(11)	0.1450(2)	0.2365(2)	0.0862(2)	6.39(6)
O(12)	0.4277(2)	0.7067(3)	0.2921(3)	7.57(8)
N(1)	0.1714(2)	0.2930(2)	0.3644(2)	3.41(4)
N(2)	0.3081(2)	0.1446(2)	0.2878(2)	4.16(5)
N(3)	0.3881(2)	0.2324(1)	0.1686(2)	3.28(4)
N(4)	0.1762(2)	0.7619(1)	0.3305(2)	3.35(4)
N(5)	0.2268(2)	0.8250(1)	0.1509(2)	4.22(5)
N(6)	0.3033(1)	0.6659(1)	0.0443(2)	2.91(4)
N(7)	0.3626(2)	0.3473(2)	−0.1216(2)	6.27(8)

[a] U_{eq} = one-third of the trace of the orthogonalized U_{ij} tensor.

Table 3. Selected Atomic Coordinates and Equivalent Isotropic Displacement Parameters (Å^2 × 100) for $[(L^3Cu)_2Ce(NO_3)_3]$, **3Ce**

atom	*x/a*	*y/b*	*z/c*	U_{eq}[a]
Ce	0.22987(2)	0.25464(1)	0.51767(2)	3.07(1)
Cu(1)	0.01351(3)	0.10845(2)	0.55419(4)	2.97(1)
Cu(2)	0.35131(4)	0.46028(2)	0.53756(4)	3.56(1)
O(1)	0.0194(2)	0.1432(1)	0.4082(2)	3.36(5)
O(2)	0.4226(2)	0.3786(1)	0.6166(2)	3.34(5)
O(3)	0.2870(2)	0.1354(2)	0.6003(3)	3.79(5)
O(4)	0.2099(2)	0.2966(2)	0.3228(3)	4.34(6)
O(5)	0.1039(2)	0.2657(2)	0.6871(3)	4.63(6)
O(6)	0.3094(3)	0.3044(2)	0.7958(3)	4.96(6)
O(7)	0.1917(4)	0.2909(2)	0.9088(3)	7.4(1)
O(8)	0.2385(2)	0.1288(2)	0.3044(3)	4.15(5)
O(9)	0.4250(2)	0.1968(2)	0.4573(3)	4.27(5)
O(10)	0.4124(3)	0.0929(2)	0.2747(3)	5.63(7)
O(11)	0.0189(3)	0.3243(2)	0.4591(4)	6.15(8)
O(12)	0.1890(2)	0.4094(2)	0.6192(3)	4.64(6)
O(13)	0.0022(3)	0.4481(2)	0.5820(4)	8.2(1)
N(1)	−0.1691(2)	0.1033(2)	0.5096(3)	3.21(5)
N(2)	0.0140(3)	0.0730(2)	0.7041(3)	3.63(6)
N(3)	0.2004(2)	0.1133(2)	0.6445(3)	3.25(6)
N(4)	0.4430(3)	0.5602(2)	0.6967(3)	3.71(6)
N(5)	0.2916(3)	0.5393(2)	0.4451(3)	4.37(7)
N(6)	0.2339(3)	0.3801(2)	0.3558(3)	3.89(6)
N(7)	0.2024(3)	0.2879(2)	0.8007(3)	4.72(7)
N(8)	0.3597(3)	0.1381(2)	0.3433(3)	3.51(6)
N(9)	0.0667(3)	0.3952(2)	0.5542(4)	5.13(8)

[a] U_{eq} = one-third of the trace of the orthogonalized U_{ij} tensor.

Table 4. Selected Bond Lengths (Å), Distances (Å), and Angles (deg) for $[\{L^1Cu(H_2O)\}_2Gd(H_2O)(NO_3)](NO_3)_2(H_2O)_2$, **1Gd**, and for $[(L^3Cu)_2Ce(NO_3)_3]$, **3Ce**[a]

	1Gd	3Ce
$Cu-O_{phenolato}$	1.906(2)−1.911(2)	1.901(2)−1.919(2)
Cu−N(1,4)	1.946(2)−1.952(2)	1.924(3)−1.921(3)
Cu−N(2,5)	1.923(2)−1.917(2)	1.927(3)−1.934(3)
Cu−N(3,6)	1.966(2)−1.985(2)	1.968(3)−1.962(3)
$Cu-O_{water}$	2.351(2)−2.363(3)	
$Cu-O_{nitrato}$		2.526(2)−2.550(3)
$Ln-O_{nitrato}$	2.476(2)−2.562(2)	2.627(3)−2.694(3)
$Ln-O_{phenolato}$	2.371(2)−2.372(2)	2.603(2)−2.604(2)
$Ln-O_{oximato}$	2.342(2)−2.403(2)	2.486(2)−2.410(2)
$Ln-O_{methoxy}$	2.594(2)−2.620(2)	
$Ln-O_{water}$	2.416(2)	
α[b]	7.3(3)−8.8(2)	46.5(1)−45.3(1)
Ln···Cu(1)	3.6388(4)	3.6070(5)
Ln···Cu(2)	3.6328(3)	3.5967(4)

[a] Ln = Gd for **1Gd** and Ce for **3Ce**. [b] Dihedral angle between O−Ln−O and N−Cu−O planes.

Bound and unbound nitrato ions and water molecules are involved in an extensive network of hydrogen bonds possibly leading to a small shortening of the intermolecular Gd···Gd ($1-x, 1-y, -z$) distance (5.9996(3) Å). Other intermolecular Gd···Cu, Gd···Gd, and Cu···Cu separations are larger than ca. 6.4 Å, while the Cu(1)...Cu(2) distance within the trinuclear entity is equal to 6.3867(4) Å.

Finally, the two halves (L^1Cu)Gd/2 of **1Gd** offer many similarities to each other and to their binuclear analogue **1′Gd**.[1] The related bond lengths and angles are not fundamentally different. We note that the dihedral angle α characterizing the bridging network scarcely varies from 7.3(3)° and 8.8(2)° in **1Gd** to 6.1(3)° in **1′Gd** while the related Cu···Gd distance decreases from 3.6388(4) and 3.6328(3) Å to 3.6210(3) Å. The major differences between the trinuclear and binuclear complexes originate in the nature of the actual polynuclear species (cationic vs neutral) and the coordination number of the gadolinium ion (nine vs ten).

Description of the 3Ce Structure. We have failed to obtain well-shaped crystals of the gadolinium complex **3Gd**, but we have succeeded in doing so for the isomorphous cerium complex $(L^3Cu)_2Ce(NO_3)_3$ **3Ce**.[29] The unit cell contains four trinuclear entities without any neutral molecule (water or organic solvent). Each entity is neutral and has no crystallographic symmetry. One molecular unit is represented in Figure 3, while relevant bond distances and angles are reported in Table 4.

The two (L^3Cu)Ce/2 halves which form the molecular unit are not identical, but the bond length differences are small. The largest one (0.076 Å) affects the bond between the cerium ion and the oximato oxygen atom. The other differences in the Ce(III) and Cu(II) environments are at the best equal to 0.030 Å. An unexpected feature of the structure is that the cerium ion is triply connected with each copper ion. In addition to the usual (O, N−O) bridging pathways, a third bridge is afforded by a bidentate NO_3 ion. In each (Cu−Ce) pair, an axial position of Cu(II) is occupied by a nitrato oxygen atom (O(5) or O(12)) which is already linked to Ce(III). This third bridge is likely responsible for the shortening of the intramolecular Cu···Ce distances (3.6070(5) and 3.5967(4) Å) compared to the value (3.6753(6) Å) observed for the related binuclear complex $L^1Cu(H_2O)Ce(H_2O)(NO_3)_3$ **1′Ce**.[30] However, it may be underlined that, in contrast to the main bridging network Cu(O,N−O)Ce, the NO_3 bridge in **3Ce** is not able to mediate any significant intermetallic interaction. Indeed, it concerns an axial position of the copper(II) ion which possesses a vanishingly small spin density. The five atoms of each Cu(O,N−O)Ce framework are far from being coplanar. The dihedral angle α between the (OCuN) and (OCeO) planes takes the values 46.5(1)° (Cu(1)) and 45.3(1)° (Cu(2)) which are not very different from the value (39.1(1)°) observed in **2′Gd**[1] but much larger than those found in **1′Gd** (6.1(3)°)[1] and **1′Ce**.[30]

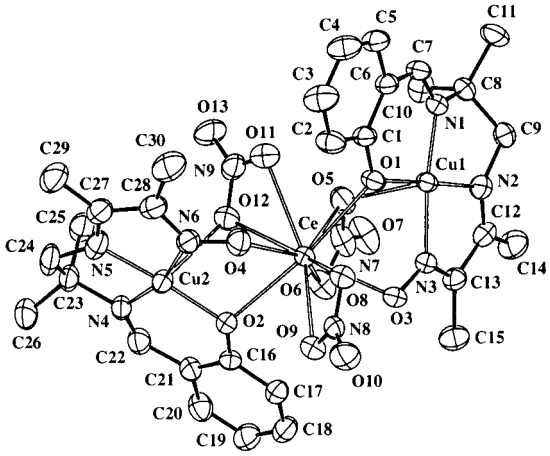

Figure 3. Zortep plot for **3Ce** with ellipsoids drawn at the 50% probability level.

The intramolecular Cu(1)···Cu(2) separation of 7.0149(6) Å is within the normal range of values for polynuclear (Cu−Ln) complexes. By contrast, abnormally small values of 3.4417(6) and 3.989(1) Å are observed for the intermolecular Cu(1)···$Cu(1)_i$ and Cu(2)···$Cu(2)_j$ distances respectively, *i* and *j* standing here for the ($-x, -y, 1-z$) and ($1-x, 1-y, 1-z$) symmetry operations. Regarding the possibilities of magnetic interaction, one may note that in both cases the Cu···$Cu_{i,j}$ vector is almost perpendicular to the related equatorial coordination planes and therefore does not mediate any significant magnetic interaction. Furthermore the axial sites of the Cu(II) ions are known to support vanishingly small spin densities.

Both copper(II) ions are five-coordinated. As expected, the axial Cu−O bonds involved in the nitrato bridges are longer (mean value 2.538 Å) than the equatorial Cu−O (mean value 1.910 Å) and Cu−N (mean value 1.939 Å) bonds. The lanthanide ion is 10-coordinated. In addition to the four oxygen atoms afforded by two monometallic units (L^3Cu), Ce(III) completes its surrounding with six oxygens from three bidentate NO_3 anions. Out of these six oxygen atoms, two are also linked to a Cu(II) ion (see above). The shortest lanthanide−oxygen bonds (2.410(2) and 2.486(2) Å) are issued from the oximato groups. The lengths of the other Ce−O bonds vary from 2.603(3) to 2.694(3) Å, the largest values being related to the bonds involving the nitrato anions.

In the series of complexes formed by L^4Cu and rare earth ions, the lack of suitable crystals prevents any structural determination to be made. The data from chemical analysis and mass (FAB^+) spectroscopy suggest that the structure of these complexes does not comprise any solvent (organic or water molecules) linked to the metal ions. They probably have structural features similar to those of $(L^3Cu)_2Ce(NO_3)_3$, each pair of metal ions (Cu, Ln) involving a triple bridge and large values of the dihedral angle between the two halves of the main bridging pathway Cu(O,N−O)Ln.

Magnetic Study. The magnetic study concerns the (Cu, La, Cu) and (Cu, Gd, Cu) triads to which a spin-only formalism

(29) Powder diffraction spectra establish an isomorphism relationship for **3Ce** and **3Gd**.

(30) The structural data characterizing **1′Ce** will be published elsewhere. However, it is interesting to note that **1′Ce** and **1′Gd** are isomorphous.

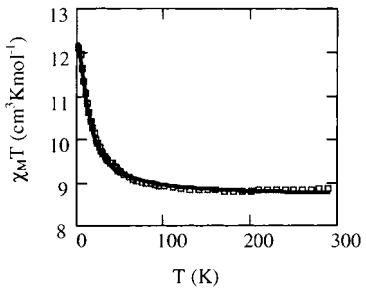

Figure 4. Thermal dependence of $\chi_M T$ for **1Gd** at 0.1 T. The full line corresponds to the best data fit.

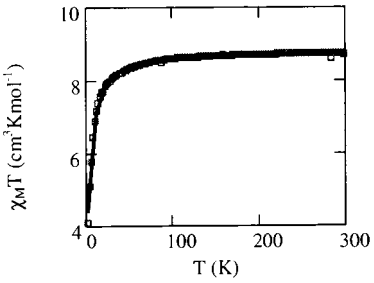

Figure 5. Thermal dependence of $\chi_M T$ for **3Gd** at 0.1 T. The full line corresponds to the best data fit.

may be applied. Indeed La^{III} with a $^1S_0$ ground state is diamagnetic while Gd^{III} with a $^8S_{7/2}$ ground state is devoid of first-order angular momentum.

Two (Cu, La, Cu) complexes are available, **3La** and **4La**. The related complex **1La** cannot be prepared. For **3La**, the thermal dependence of $\chi_M T$ is characteristic of a small antiferromagnetic interaction since no maximum appears in the χ_M vs T curve until 2 K. Least-squares fit of the experimental data with the equation valid for a copper(II) pair[31] leads to $J_{CuCu} = -1.8$ cm^{-1}. The interaction is also antiferromagnetic in **4La**, but its magnitude is much smaller $|J_{CuCu}| \leq 0.1$ cm^{-1}.

In keeping with the occurrence of two types of intramolecular interactions, the analysis of the magnetic properties of (Cu, Gd, Cu) triads is based on the Hamiltonian $H = -2J_{CuGd}S_{Cu}S_{Gd} - J'_{CuCu}S_{Cu}S_{Cu}$. It is assumed that the terminal copper centers are equivalent. The energies $E(S,S')$ of low-lying spin states can be expressed as[2,9,32]

$$E(^9/_2,1) = 0; \quad E(^7/_2,1) = 9J_{GdCu}/2;$$
$$E(^7/_2,0) = 7J_{GdCu}/2 + J'_{CuCu}; \quad E(^5/_2,1) = 8J_{GdCu}$$

($^7/_2$,1) and ($^7/_2$,0) refer to the states resulting from the coupling of S_{Gd} with $S' = 1$ and 0, respectively, S' being the intermediate spin obtained by coupling the two S_{Cu}.

The temperature dependence of the experimental values of the product $\chi_M T$ (Figures 4 and 5) clearly differentiates **1Gd** from **3Gd** and **4Gd**. For the three complexes $\chi_M T$ is constant from 300 to ca. 100 K and corresponds to the value (8.6 cm^3 K mol^{-1}) anticipated for three uncoupled ions. As the temperature is lowered further, $\chi_M T$ for **1Gd** increases regularly to reach a value consistent with a $^9/_2$ spin state at 2 K while, for **3Gd** and **4Gd**, $\chi_M T$ decreases. The values observed at 2 K are slightly larger than expected for a $^5/_2$ spin state, indicating that higher spin state(s) may be operative in addition to the antiferromagnetic ground state. This point will be considered later, but it does not invalidate the conclusion that the behaviors of the three complexes are essentially dependent on interactions between the Gd^{III} and Cu^{II} ions. These interactions are ferromagnetic in **1Gd** and antiferromagnetic in **3Gd** and **4Gd**.

Table 5. Parameters Deduced from the Magnetic Susceptibility Data of the Different Complexes

	J_{CuGd} (cm^{-1})	J'_{CuCu} (cm^{-1})	g_{Cu}	g_{Gd}	R^a
1Gd	2.5	0	2.10	1.99	5×10^{-5}
3Gd	-1.8_5	0	2.10	2.01	4×10^{-5}
4Gd	−1.0	0	2.10	2.02	7×10^{-5}
1′Gd[b]	3.5		2.05	1.99	1×10^{-4}
2′Gd[b]	−0.5		2.11	1.99	5×10^{-5}

[a] $R = \Sigma[(\chi_M T)_{obs} - (\chi_M T)_{calc}]^2/\Sigma[(\chi_M T)_{obs}]^2$. [b] Cf. ref 1.

From the energies $E(S,S')$ reported above and the equations relating local and molecular g values,[33] it is straightforward to express the magnetic susceptibility as a function of T and four parameters,[2,9] J_{CuGd}, J_{CuCu}, g_{Cu}, and g_{Gd}:

$$\chi_M T = [N\beta^2/4kT][T/(T-\theta)][A/B]$$

with

$$A = [165g_{(9/2,1)}{}^2 + 84g_{(7/2,1)}{}^2 \exp(9J/2kT) + 84g_{(7/2,0)}{}^2 \exp((7J+2J')/2kT) + 35g_{(5/2,1)}{}^2 \exp(8J/kT)] \text{ and } B = [5 + 4\exp(9J/2kT) + 4\exp((7J+2J')/2kT) + 3\exp(8J/kT)]$$

θ gauges eventual second-order effects (intermolecular coupling, zero field splitting, ...). Least-squares fit of the experimental data with the above relation leads to the values quoted in Table 5. For comparison, we have reported the parameters previously obtained for the binuclear complexes **1′Gd** and **2′Gd**. We can see that these results are very coherent, particularly for **1Gd** and **1′Gd**.

It may be noted that in the trinuclear complexes **1Gd**, **3Gd**, and **4Gd** the best fitted value for J'_{CuCu} is 0. The magnetic study of the (Cu, La, Cu) analogues confirms this result in the case of **4La** but leads to a different evaluation ($J'_{CuCu} = -1.8$ cm^{-1}) in the case of **3La**. If the **3Gd** data fit is restricted to three variables (J_{CuGd}, g_{Cu}, and g_{Gd}), the fourth parameter (J'_{CuCu}) being held equal to -1.8 cm^{-1}, we obtain $J_{CuGd} = -1.7_5$ cm^{-1}, $g_{Cu} = 2.10$, and $g_{Gd} = 2.01$ with a R factor equal to $= 4 \times 10^{-5}$. Owing to the experimental uncertainties, these values are not basically different from those reported in Table 5. The low sensitivity of χ_M on the magnitude of the Cu, Cu interaction may probably be related to the fact that all of the $E(S,S')$ energies but one, $E(^7/_2,0)$, do not depend on this interaction. From the values quoted in Table 5 we can deduce the energy spectra for the low-lying spin states of the (Cu, Gd, Cu) complexes. They are shown in Figure 6 which also contains the **3Gd** spectrum obtained with the second set of parameters. In addition to the reversal of energy levels on going from **1Gd** to **3Gd** and **4Gd**, it appears that the spectrum width is smaller for **4Gd** (8.0 cm^{-1}) than for **3Gd** (14.5 cm^{-1}) and **1Gd** (20.0 cm^{-1}) so that, in the former complex, the populations of the ($^7/_2$,0) and ($^7/_2$,1) excited spin states are not negligible. At 2 K they are equal to 7.2% and 3.5%, respectively, while that of the ($^5/_2$,1) ground state is 89%.

Additional information may be gained from an analysis of the field (H) dependence of the magnetization (M). In the case

(31) Bleaney, B.; Bowers, K. D. *Proc. R. Soc. London, Ser. A* **1952**, *214*, 451.

(32) Griffith, J. S. *Struct. Bonding (Berlin)* **1972**, *10*, 87.

(33) Bencini, A.; Gatteschi, D. In *Magneto-Structural Correlations in Exchange Coupled Systems*; Willet, R. D., Gatteschi, D., Kahn, O., Eds.; D. Reidel: Dordrecht, The Netherlands, 1985.

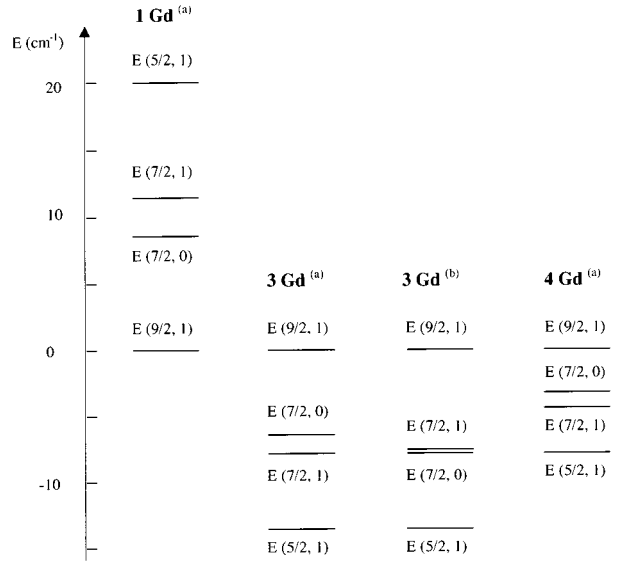

Figure 6. Energy states for the low-lying spin states of **1Gd**, **3Gd**, and **4Gd** at 2 K. $E(^9/_2,1)$ is arbitrarily taken equal to zero in the three cases. (a) Parameter values as indicated in Table 5. (b) $J_{CuGd} = -1.7_5$ cm^{-1}; $J_{CuCu} = -1.8$ cm^{-1}; $g_{Cu} = 2.10$; $g_{Gd} = 2.01$.

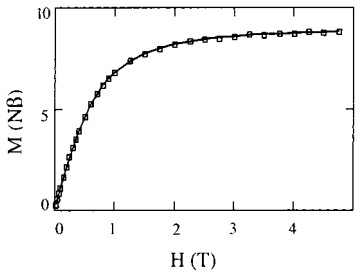

Figure 7. Field dependence of the magnetization for **1Gd**. The full line corresponds to the Brillouin function for a $S = {}^9/_2$ spin state.

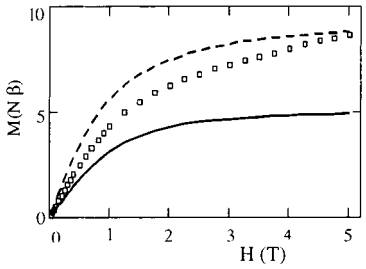

Figure 8. Field dependence of the magnetization for **4Gd**. The full line corresponds to the Brillouin function for a $S = {}^5/_2$ spin state and the dotted line to the Brillouin function for three isolated spins.

of **1Gd** the variation of M vs H at 2 K (Figure 7) is very similar to those previously reported for ferromagnetically coupled (Cu, Gd) pairs.[1,12,34] It nicely follows the Brillouin function (abbreviated as B.f.($^9/_2$) in the following) for a $S_T = {}^9/_2$ spin state and thus confirms the ferromagnetic nature of the Cu, Gd interaction in **1Gd**.

For **3Gd** and **4Gd**, the M vs H plots are linear in the low-field regime ($H \leq 0.8 \times 10^4$ G). They are in agreement with the zero-field susceptibility values determined independently. The experimental values of the magnetization obtained for **4Gd** in the field range ($(0-5) \times 10^4$ G) are represented in Figure 8 together with the theoretical curves corresponding to the Brillouin functions for a $S = {}^5/_2$ state and three uncoupled spins (S_{Gd} and two S_{Cu}), respectively, at 2 K. The magnetization increases less than expected for uncorrelated ions, confirming the antiferromagnetic nature of the interaction. However, the experimental points are located above the B.f.($^5/_2$) plot. When the field is raised, the difference between the two sets of values increases and the magnetization approaches the value anticipated for three uncoupled spins. This behavior is presumably due to two factors which converge on enlarging the participation of spin states higher than $^5/_2$. These factors are the presence of excited spin states close in energy to the ground state (cf. Figure 6) and the decoupling effect of the magnetic field. Thus the magnetization at 2 K and $H = 0.5 \times 10^4$ G would be approximated by the sum of the contributions supplied by respectively the (Cu, Gd, Cu) triads in the $S_T = {}^5/_2$ state (relative population of ca. 80%), the triads with $S_T = {}^7/_2$ (ca. 11%), and the triads comprising noninteracting spins (ca. 9%). The resulting value of 2.2 μ_B compares reasonably with the measured value of 2.4 μ_B. Similar comments can be made for **3Gd**. In this complex the difference between the observed magnetization and the values calculated for a $S_T = {}^5/_2$ state are smaller than in the case of **4Gd** in accordance with a larger gap between the ground and excited states (Figure 6) and a larger magnitude of the antiferromagnetic interaction (1.8 vs 1.0 cm^{-1}).

A point we wish to emphasize concerns the possible relationship between the magnetic properties of the (Cu, Gd) pairs and the bending of the bridging network. If we consider the values of the dihedral angle α between the (OCuN) and (OGdO) planes, it appears that the ferromagnetism of the Cu−Gd entities in **1Gd** and **1′Gd** ($J = 2.5$ and 3.5 cm^{-1}, respectively) tallies with small α values (7.3(3)°, 8.8(2)°, and 6.1(3)°, respectively). Conversely, large α values (from ca. 40° to 46°) characterize **2′Gd** and **3Gd** (judging by the isomorphous **3Ce** complex), which display antiferromagnetic Cu−Gd interactions (J from -0.5 to -1.8 cm^{-1}).

The ferromagnetic behavior of the (Cu−Gd) pair has been attributed[9,13,35] to coupling between the electronic ($3d_{Cu}-4f_{Gd}$) ground configuration and the excited configuration arising from a $3d_{Cu}-5d_{Gd}$ electron transfer. In any case this mechanism stabilizes the resulting $S = 4$ spin state with respect to the $S = 3$ one. However, the experimental data obtained for complexes with a (CuO_2Gd) core show that, as the dihedral angle α becomes larger, the magnitude of the interaction decreases and tends to vanish when α approaches a value of the order of 40°.[34] It is not unrealistic to assume that for **2′Gd**, **3Gd**, and **4Gd** the ferromagnetic contribution is reduced to such an extent that an underlying weak antiferromagnetism becomes perceptible. To account for this antiferromagnetism, two mechanisms are available: the Heitler−London type interaction[9,36,37] and/or the Anderson mechanism.[9,38,39] In the former approach the antiferromagnetism of a (Cu−Gd) pair would arise in the ground configuration ($3d_{Cu}-4f_{Gd}$) from overlap between natural orbitals. The latter model is based on the interaction between the ground configuration and the excited configurations corresponding to either the 3d → 4f or the 4f → 3d metal−metal charge transfer, both leading to an $S = 3$ excited-pair state. The Heitler−London mechanism and the Anderson one have been assumed[9] to be

(34) Costes, J. P.; Dahan, F.; Dupuis, A.; Laurent, J. P. *Inorg. Chem.* **2000**, *39*, 165.

(35) Goodenough, J. B. In *Magnetism and the Chemical Bond*; Interscience: New York, 1963.

(36) Kahn, O. In *Magneto-Structural Correlations in Exchange Coupled Systems*; Willet, R. D., Gatteschi, D.; Kahn, O., Eds.; D. Reidel: Dordrecht, The Netherlands, 1985.

(37) Girerd, J. J.; Charlot, M. F.; Kahn, O. *Chem. Phys. Lett.* **1981**, *82*, 534.

(38) Anderson, P. W. *Phys. Rev.* **1956**, *115*, 2.

(39) Anderson, P. W. In *Magnetism*; Rado, G. T., Suhl, H., Eds.; Academic Press: NewYork, 1963; Vol. 1, Chapter 2.

inoperative in the complexes built around a CuO_2Gd core. It has been stated that, due to the contraction of the 4f orbital around the gadolinium nucleus and their shielding by the 6s and 5p orbitals, all the integrals involving a 4f−3d density would vanish. In the case of complexes **2′Gd**, **3Gd**, and **4Gd** the observed antiferromagnetism demands that the Heitler−London interaction and/or the Anderson one become operative, implying that the total 4f−3d overlap density takes a finite value.

Acknowledgment. We thank Dr. A. Mari for his contribution to the magnetic measurements and Dr. S. Richelme (Service Commun de Spectroscopie de Masse) for her contribution to the mass spectra data. The authors are greatly indebted to Dr. J. P. Laurent for fruitful discussion and comments.

Supporting Information Available: X-ray crystallographic files including the structural data for $[\{L^1Cu(H_2O)\}_2Gd(H_2O)(NO_3)](NO_3)_2(H_2O)_2$ **1Gd** and for $[(L^3Cu)_2Ce(NO_3)_3]$ **3Ce** in CIF format. This material is available free of charge via the Internet at http://pubs.acs.org.

IC000666U